Stabilization of triple-helical structures of collagen peptides containing a Hyp-Thr-Gly, Hyp-Val-Gly, or Hyp-Ser-Gly sequence

ARTICLE *in* BIOPOLYMERS · SEPTEMBER 2011

Impact Factor: 2.39 · DOI: 10.1002/bip.21625 · Source: PubMed

6 AUTHORS, INCLUDING:

Kenji Okuyama
Osaka University
192 PUBLICATIONS **3,274** CITATIONS
SEE PROFILE

Kazunori Mizuno
Nippi Inc.
47 PUBLICATIONS **693** CITATIONS
SEE PROFILE

Hans Peter Bächinger
Shriners Hospitals for Children
162 PUBLICATIONS **8,282** CITATIONS
SEE PROFILE

Stabilization of Triple-Helical Structures of Collagen Peptides Containing a Hyp-Thr-Gly, Hyp-Val-Gly, or Hyp-Ser-Gly Sequence

Kenji Okuyama,[1] Keita Miyama,[1] Tatsuya Morimoto,[1] Kouichi Masakiyo,[1] Kazunori Mizuno,[2] Hans Peter Bächinger[2,3]

[1] *Department of Macromolecular Science, Graduate School of Science, Osaka University, Osaka 560-0043, Japan*

[2] *Research Department, Shriners Hospital for Children, Portland, OR 97239*

[3] *Department of Biochemistry and Molecular Biology, Oregon Health & Science University, Portland, OR 97239*

Received 5 January 2011; revised 7 March 2011; accepted 7 March 2011
Published online 25 March 2011 in Wiley Online Library (wileyonlinelibrary.com). DOI 10.1002/bip.21625

ABSTRACT:

The single-crystal structures of three collagen-like host–guest peptides, (Pro-Pro-Gly)$_4$-Hyp-Yaa-Gly-(Pro-Pro-Gly)$_4$ [Yaa = Thr, Val, Ser; Hyp = (4R)-4-hydroxyproline] were analyzed at atomic resolution. These peptides adopted a 7/2-helical structure similar to that of the (Pro-Pro-Gly)$_9$ peptide. The stability of these triple helices showed a similar tendency to that observed in Ac-(Gly-Hyp-Yaa)$_{10}$-NH$_2$ (Yaa = Thr, Val, Ser) peptides. On the basis of their detailed structures, the differences in the triple-helical stabilities of the peptides containing a Hyp-Thr-Gly, Hyp-Val-Gly, or Hyp-Ser-Gly sequence were explained in terms of van der Waals interactions and dipole–dipole interaction between the Hyp residue in the X position and the Yaa residue in the Y position involved in the Hyp(X):Yaa(Y) stacking pair. This idea also explains the inability of Ac-(Gly-Hyp-alloThr)$_{10}$-NH$_2$ and Ac-(Gly-Hyp-Ala)$_{10}$-NH$_2$ peptides to form triple helices. In the Hyp(X):Thr(Y), Hyp(X):Val(Y), and Hyp(X):Ser(Y) stacking pairs, the proline ring of the Hyp residues adopts an up-puckering conformation, in agreement with the residual preference of Hyp, but in disagreement with the positional preference of X in the Gly-Xaa-Yaa sequence. © *2011 Wiley Periodicals, Inc. Biopolymers 95: 628–640, 2011.*

Keywords: collagen; crystal structure; protein stability; triple helix; threonine

This article was originally published online as an accepted preprint. The "Published Online" date corresponds to the preprint version. You can request a copy of the preprint by emailing the Biopolymers editorial office at biopolymers@wiley.com

INTRODUCTION

Collagens are a family of extracellular matrix proteins that are found in all connective tissues. They are the most abundant group of proteins in multicellular animals, and collagens of both vertebrates and invertebrates share the same characteristic Gly-Xaa-Yaa tripeptide repeating unit, which is essential for the formation of the collagen triple helix. Most of the collagen in animals is in a fibrillar form (e.g., Types I, II, or III), in which each collagen molecule is ~3000 Å long and is staggered by 670 Å with respect to its neighbor.

The collagen helix is stabilized by high contents of imino acid residues and by hydrogen bonds between the NH groups of Gly residues and the C=O groups of Xaa residues in adjacent chains. In addition to these, hydroxylation of Pro residues in the Y position is essential for stable formation of a triple helix and, hence, for regular fiber formation. Because the helix–coil transition temperature (T_m) of (Pro-Hyp-Gly)$_{10}$ [Hyp = (4*R*)-4-hydroxyproline] is higher than that of (Pro-Pro-Gly)$_{10}$ by about 30°C, and because (Hyp-Pro-Gly)$_{10}$ cannot form a triple-helical conformation under aqueous conditions,[1] it was believed for 2 decades that a Hyp residue

Correspondence to: Kenji Okuyama; e-mail: okuyamak@chem.sci.osaka-u.ac.jp

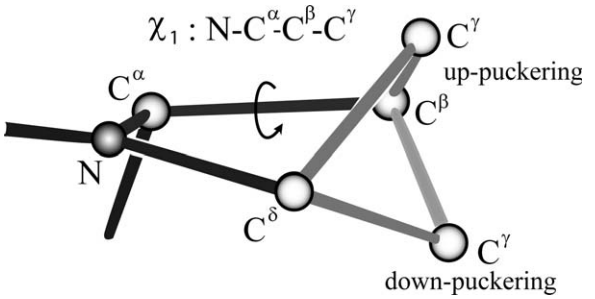

FIGURE 1 The two puckering conformations of a proline ring: up-puckering (C^{γ}-exo) and down-puckering (C^{γ}-endo).

in the Y position stabilizes the triple-helical conformation, whereas a Hyp residue in the X position destabilizes it.

The side chain of the proline ring adopts one of two conformations: an up-puckering (C_{γ}-exo) conformation or a down-puckering (C_{γ}-endo) conformation. These are defined by negative and positive values of the χ_1 angle ($<NC_{\alpha}C_{\beta}C_{\gamma}$), respectively (see Figure 1). As observed in many protein and peptide structures in databases (PDB[2] and CSD[3]), Pro residues adopt both up- and down-puckering conformations, whereas Hyp residues adopt an up-puckering conformation preferentially.[4] This tendency is called the "residual preference" or "intrinsic preference." In the collagen helix, however, the X and Y positions in the Xaa-Yaa-Gly sequence preferentially adopt down- and up-puckering conformations, respectively.[4] This preference for residues in the X and Y positions is called "positional preference." On the basis of the intrinsic preference of individual imino acids and the positional preference in the X and Y positions, Vitagliano et al. proposed the propensity-based hypothesis,[4] which nicely explains the position-sensitive stabilization and destabilization induced by Hyp. However, it does not explain some recent experimental observations, such as the formation of a stable triple helices by peptides with Hyp-Hyp-Gly,[5–7] Hyp-Thr-Gly, or Hyp-Val-Gly sequences.[8]

In the collagen helix, each peptide strand must be staggered by one residue with respect to its neighbor to ensure that every glycine residue can localize near the helical axis. Because of this one-residue stagger, three amino acid residues, Xaa from the first, Yaa from the second, and Gly from the third strands, are at similar locations along the helical axis (see Figure 2). Since each strand has a coiled-coil conformation, the distances between side chain atoms of Xaa and Yaa residues are, in some cases, close enough for an attractive interaction. We call these two residues a "stacking pair." For example, in the DEF-molecule (Figure 2a), residues Hyp13D and Val14F, Hyp13E and Val14D, Pro16F and Val14E, and Pro16D and Pro17F are stacking pairs.

The contribution made by van der Waals interactions between stacking pairs to the stability of the triple-helical structure of $(Pro\text{-}Pro\text{-}Gly)_{10}$ was first suggested by Bhatnagar et al.[9] on the basis of their molecular mechanics calculations. In a study of $(Pro\text{-}Pro\text{-}Gly)_9$, Hongo et al. pointed out that this van der Waals interaction is most effective when Pro(X) and Pro(Y) residues adopt down- and up-puckering conformations, respectively.[10] These puckering conformations in the X and Y positions match the propensity-based hypothesis[4]; this suggests that the physical basis of this hypothesis may originate from the Pro(X):Pro(Y) stacking interaction. In discussing the stability of the triple helix, we therefore focused on the stability induced by the stacking interaction rather than on the amino acid sequence.

In our previous publication,[11,12] we studied the puckering conformation of Hyp at the X position in Hyp(X):Yaa(Y) stacking pairs of host–guest peptides $(Pro\text{-}Pro\text{-}Gly)_4\text{-}Xaa\text{-}Yaa\text{-}Gly\text{-}(Pro\text{-}Pro\text{-}Gly)_4$, where (Xaa, Yaa) = (Hyp, Pro), (Pro, *allo*Hyp), or (Hyp, Hyp) [*allo*Hyp = (4*S*)-4-hydroxyproline; Hyp enantiomer]. In summary, we found that Hyp(X) residues involved in Hyp(X):Pro(Y) stacking pairs prefer down-puckering, despite their intrinsic preference, whereas Hyp(X) residues involved in Hyp(X):Hyp(Y) stacking pairs prefer up-puckering, despite the positional preference.[12]

Almost all proline residues in the Y positions of vertebrate collagens are post-translationally modified by prolyl-4-hydroxylase to form (4*R*)-4-hydroxyproline residues. However, in the case of an invertebrate collagen, the cuticle collagen from the deep-sea hydrothermal vent worm *Riftia pachyptila* exhibits unique characteristics, in that it has a relatively high thermal stability (T_m = 37°C) despite having a low content of Pro and Hyp residues (~ 5%), and it has Hyp residues in the X position.[13,14] To understand the role of Hyp residues in the X position, Mizuno et al. synthesized a series of $Ac\text{-}(Gly\text{-}Hyp\text{-}Yaa)_{10}\text{-}NH_2$ (Yaa = Thr, Ala, Ser, Val, *allo*Thr) peptides, where *allo*Thr is (3S)-threonine, an enantiomer of Thr. They found that in water, only the Thr- and Val-containing peptides formed triple helices, and they hypothesized that the methyl group shields the interchain hydrogen bond between the NH group of the Gly residue and the carbonyl oxygen of the Xaa residue from water, and that the OH group of Thr can form direct or water-mediated hydrogen bonds with Hyp.[8] By using molecular dynamics (MD) simulation methods, Radmer and Klein explained the stability difference in terms of weakened hydrogen bonds that result from extended Yaa residue ψ angles that prevent the attainment of an optimal geometry for the triple-helical structure.[15]

To understand the stability difference from a structural point of view, we performed high-resolution analyses of the host–guest peptides $(Pro\text{-}Pro\text{-}Gly)_4\text{-}Xaa\text{-}Yaa\text{-}Gly\text{-}(Pro\text{-}Pro\text{-}Gly)_4$ (Yaa = Thr, Val, Ser). These peptides can be abbrevi-

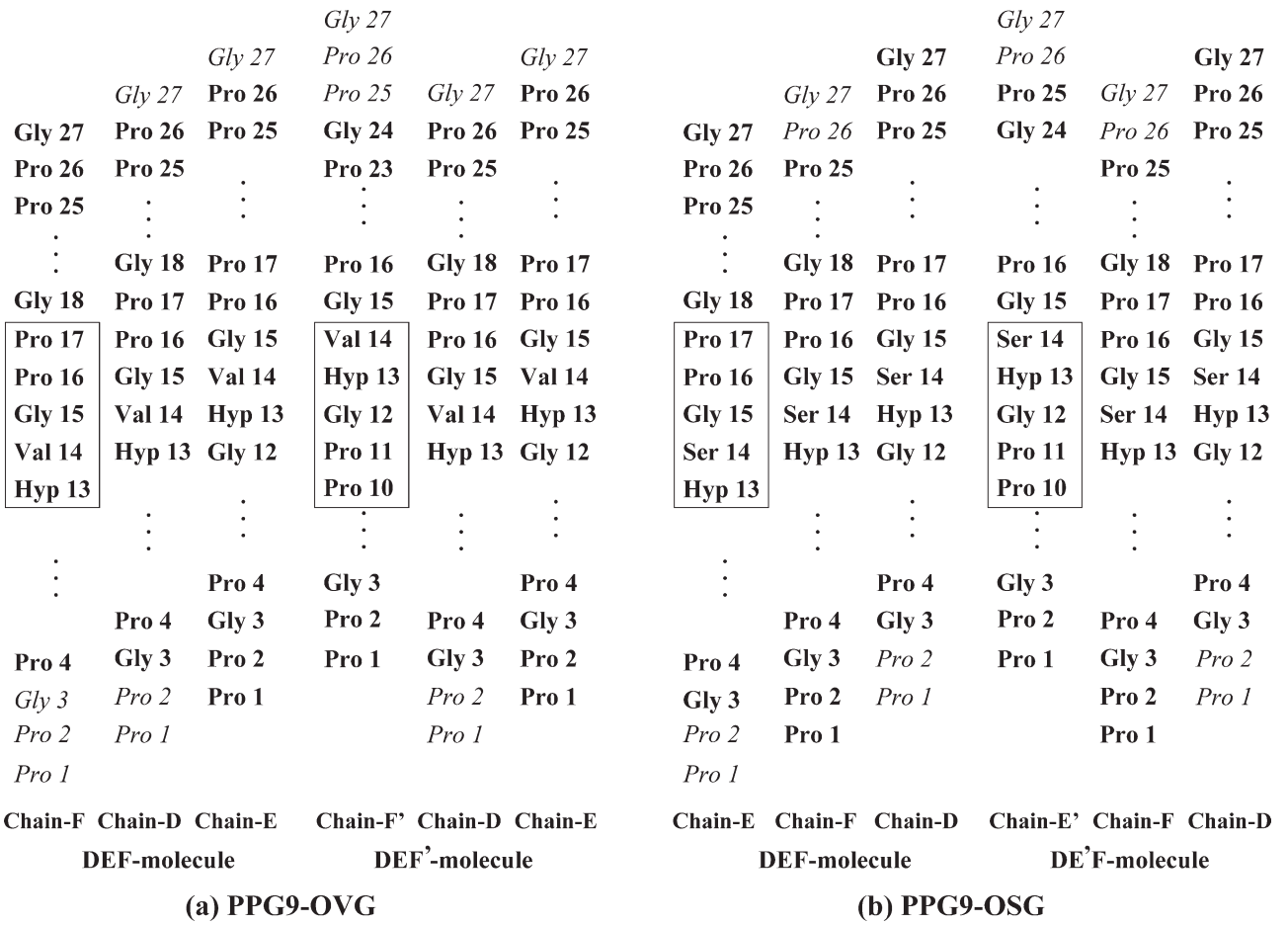

(a) PPG9-OVG (b) PPG9-OSG

FIGURE 2 Translational disorder observed in the DEF-molecules of (a) PPG9-OVG and (b) PPG9-OSG peptides. The trailing strand (chain F) of the PPG9-OVG peptide becomes the leading strand (chain F′) by shifting one triplet toward the C-terminal side. In the same manner, the trailing strand (chain E) of the PPG9-OSG peptide becomes the leading strand (chain E′) by shifting one triplet toward the C-terminus. In the structural analyses, the residues enclosed by rectangles in chains F and F′, and those in chains E and E′ were refined independently. Residues shown in italics are missing residues.

ated as PPG9-OYG, where, "O" represents (4*R*)-4-hydroxyproline (Hyp). In our previous structure analysis of PPG9-OTG,[16] we reported a *gauche*$^+$-*trans* conformation of the Thr side chain and the presence of water-mediated hydrogen-bond networks involving the hydroxy group of Thr(Y).[16] Although we were able to determine the side-chain conformation of Thr, we could not determine the puckering conformation of Hyp because of the low electron density around its C^{γ} and O^{δ} atoms. At the time, we did not suspect the possibility of crystal twinning in this peptide. However, after the initial discovery of crystal twinning in an analysis of PPG9-OVG, we recognized that PPG9-OTG also exhibits crystal twinning. In the present study, therefore, the PPG9-OTG crystal was reanalyzed by using newly obtained single crystals under the twinning conditions. We were able to improve the quality of the structural analysis; the completeness was increased from 92.9% to 97.4%, the resolution from 1.15 Å to 1.08 Å, and the R/R_{free} ratio from 0.23/0.32 to 0.14/0.19, but otherwise there are no important differences from our previous report.[16]

METHODS

Peptide Syntheses and Purification

Peptides were synthesized by using an ABI 433A synthesizer (Applied Biosystems, Foster City, CA). HATU {*N*-[(dimethylamino)(3*H*-[1,2,3]triazolo[4,5-*b*]pyridin-3-yloxy)methylene]-*N*-methylmethanaminium hexafluorophosphate (Perseptive Biosystems) (4.0 eq.)} and ethyl(diisopropyl)amine were used as the coupling reagents for the Fmoc solid-phase peptide synthesis. The

Table I Crystallization Conditions

	PPG9-OTG	PPG9-OVG	PPG9-OSG
Crystallization method	Sitting drop	Hanging drop	Hanging drop
Crystallization temperature	277 K	277 K	277 K
Peptide solution	20 mg/ml peptide 0.1 M MES[a] buffer	6.0 mg/ml peptide	4.0 mg/ml peptide
Reservoir solution	25% (w/v) PEG400[b] 0.1 M MES buffer pH 5.9	22.5% (w/v) PEG2000 0.1 M acetate buffer pH 5.6	22.5% (w/v) PEG2000 0.1 M acetate buffer pH 5.6
Cryoprotectant	–	30% (w/v) MPD[c]	25% (w/v) MPD
Crystallization term	3 days	1 month	2–3 weeks

[a] MES = 2-morpholin-4-ylethanesulfonic acid.
[b] PEG = poly(ethylene glycol): the figures denote the average molecular weight.
[c] MPD = 2-methylpentane-2,4-diol.

peptides were cleaved from the resin with Reagent R [a 90:5:3:2 mixture of trifluoroacetic acid, (methylsulfanyl)benzene, ethane-1,2-dithiol, and methoxybenzene] at room temperature for 3 h. Peptides were isolated by precipitation from the cleavage cocktail with diethyl ether at 4°C. They were then dissolved in 0.1% trifluoracetic acid (TFA), and purified by preparative HPLC (Vydac® C18, 5 μm, 300 Å, 218TP101550, 50 × 250 mm; guard column: 218TP15202503, W.R. Grace & Co., MD) with a flow-rate of 36 ml/min and elution by a 0–50% gradient of acetonitrile in 0.1% aqueous TFA. All the peptides were characterized by electrospray/quadrupole/time-of-flight mass spectrometry (Q-tof micro, Waters Corp., MA), and by amino acid analysis. The peptides were stored at −20°C before making stock solutions. The stock solutions for the analysis were stored at 4°C.

Circular Dichroism Spectroscopy

Circular dichroism (CD) spectra of PPG9-OTG, PPG9-OVG, and PPG9-OSG peptides were recorded on an Aviv 202 spectropolarimeter (AVIV Biomedical, Lakewood, NJ) using a Peltier thermostatted cell holder and a rectangular quartz cell with a path length of 1 mm (Starna Cells, Atascadero, CA). Measurements were performed in phosphate-buffered saline (PBS) at a peptide concentration of 1 mg/ml. Peptide concentrations were determined by amino acid analysis (L-8800A, Hitachi High Technologies America, San Jose, CA). The temperature-scanning experiments were performed at 6°C/h.

Crystallization and Data Collection

The purified and lyophilized peptides were crystallized at 277 K by either the sitting-drop (PPG9-OTG) or the hanging-drop (PPG9-OVG and PPG9-OSG) vapor-diffusion methods. For crystallization, 2 μl of the peptide solution was mixed with 2 μl of the reservoir solution, which produced rectangular single crystals. The resulting crystals were dipped in a mixture of the cryoprotectant 2-methylpentane-2,4-diol (MPD) and the same volume of reservoir solution for several seconds, before flash freezing. Details of the crystallization conditions are summarized in Table I, and details of the data collection are listed in Table II.

Diffraction data sets for the PPG9-OVG and PPG9-OSG crystals were measured on the BL44XU beamline at SPring-8, and the diffraction images of these data were processed by using *HKL*-2000.[17] The diffraction data set for the PPG9-OTG crystal was measured on the BL41XU beamline at SPring-8, and the diffraction images were processed by using CrystalClear software (Rigaku, Tokyo). The PPG9-OTG and PPG9-OVG crystals exhibited pseudo-merohedral twinning, with twin fractions of 0.44 and 0.40, respectively, as estimated from the *H* plot produced by *phenix.xtriage*.[18] The twin law was shown to be (*h, –k, –l*) in both cases. Pseudo-merohedral twinning has been frequently observed in crystals of host–guest peptides with (Pro-Pro-Gly)$_4$-Xaa-Yaa-Gly-(Pro-Pro-Gly)$_4$ sequences.[12]

Structure Determination and Refinement

The initial phases of these three crystals were obtained by using the Phaser program[19] with the triple-helical structure of (Pro-Pro-Gly)$_9$ (PDB code 2CUO)[10] as a probe. For the PPG9-OTG and PPG9-OVG peptides, the detwinned data sets were used in this calculation. The obtained structures were refined by using the SHELXL program.[20] The structures of the PPG9-OTG and PPG9-OVG peptides were refined under the twinning operator (*h, –k, –l*). The refinement statistics are listed in Table II. During the structural analyses, Coot[21] was used for visualization of the structures, and the figures were generated by using MolFeat (FiatLux Co., Tokyo). Helical parameters were calculated by using the in-house program PHEL. Coordinates and structure factors have been deposited in the Protein Data Bank with the accession codes 3A1H (PPG9-OTG), 3A0M (PPG9-OVG), and 3ADM (PPG9-OSG).

RESULTS AND DISCUSSION

Triple-Helix Stability of PPG9-OYG Peptides

The triple-helix–coil transition temperature (T_m) of Ac-(Gly-Hyp-Yaa)$_{10}$-NH$_2$ peptides in propane-1,2-diol and propane-1,3-diol decreased in the order Ac-(Gly-Hyp-Thr)$_{10}$-NH$_2$ > Ac-(Gly-Hyp-Val)$_{10}$-NH$_2$, > Ac-(Gly-Hyp-Ser)$_{10}$-NH$_2$ (Table III).[8] In water, the first two peptides formed a triple-helical structure whereas the third did not do so (Table III). This tendency was retained in the present host–guest peptides,

Table II Data Collection and Refinement Statistics

Peptide	PPG9-OTG	PPG9-OVG	PPG9-OSG
A. Data Collection			
Facility	SPring-8	SPring-8	SPring-8
Beamline	BL41XU	BL44XU	BL44XU
Data-collection device	ADSC Quantum 315	DIP6040	DIP6040
Data-collection temperature (K)	100	100	100
Wavelength (Å)	1.0	0.70	0.90
Resolution (Å)	26.5–1.08	24.8–0.98	50.0–1.18
(last shell)	1.12–1.08	1.02–0.98	1.20–1.18
Number of unique reflections	46,090	60,025	34,897
Overall completeness (%)	97.4	97.0	96.1
(last shell)	99.1	98.1	70.6
R_{merge} (last shell)	0.08 (0.30)	0.05 (0.35)	0.05 (0.31)
Redundancy (last shell)	3.3 (3.3)	2.6 (2.6)	3.3 (2.5)
$\langle I_0/\sigma(I_0)\rangle$	7.0 (2.9)	10.5 (3.1)	11.4 (3.3)
Twin fraction	0.44	0.40	–
Space group	$P2_1$	$P2_1$	$P2_1$
Unit cell dimensions			
a (Å)	25.99	26.12	26.52
b (Å)	26.49	26.37	26.10
c (Å)	80.21	79.94	79.67
β (°)	89.85	90.08	91.57
B. Structure Refinement			
Final twin fraction	0.494	0.385	–
Twin law	$h, -k, -l$	$h, -k, -l$	–
Resolution range (Å)	26.5–1.08	24.8–1.02	50.0–1.18
Data cutoff for refinement [$\sigma(I_0)$]	3.0	0.0	0.0
No. of reflections for refinement	43,250	51,506	33,143
No. of reflections for R_{free}	2279	2698	1745
R	0.135	0.116	0.166
R_{free}	0.185	0.143	0.214
No. of refined parameters	9,778	10,851	11,326
Max/Min. peaks in D-maps (e/Å^3)	0.36/–0.41	0.52/–0.38	0.50/–0.32
No. of peptide nonhydrogen atoms	864	929	1106
No. of water sites	222	280	280
RMS deviations from standard geometry			
Bonds (Å)	0.014	0.014	0.008
Angles (Å)	0.034	0.029	0.024
Planes (Å)	0.037	0.032	0.031
Atomic displacement parameters (Å^2)			
Peptide atoms	10.7	10.9	15.3
Water oxygen atoms	16.1	18.0	25.2
PDB code	3A1H	3A0M	3ADM

PPG9-OTG, PPG9-OVG, and PPG9-OSG. We therefore expected that the same stabilization and destabilization mechanism should control the triple-helix stability of the host–guest peptides and that of the homopeptides. Because, despite protracted efforts, we could not obtain single crystals of Ac-(Gly-Hyp-Thr)$_{10}$-NH$_2$ or (Gly-Hyp-Thr)$_{10}$, we used the host–guest peptides with the PPG9-OYG (Y = Thr, Val, Ser) to understand the above stability difference on the basis of their three-dimensional structures.

Translational Disorder Along the Helical Axis

In the triple-helical structure of collagen, peptides are staggered by one residue between adjacent strands; this ensures

Table III Triple-Helix–Coil Transition Temperatures (T_m) of Peptides Containing a Hyp-Thr-Gly, Hyp-Val-Gly, or Hyp-Ser-Gly Sequence

	T_m (°C)			
Y	*T*	*a*T [a]	*V*	*S*
Ac-$(GOY)_{10}$-NH_2 [8]				
In propane-1,2-diol	48	38	33	27
In propane-1,3-diol	56	43	47	ns [b]
In water	18	<4	~ 18	<4
PPG9-OYG				
In PBS [c]	16	–	16	10

[a] *a*T = *allo*Thr, an enantiomer of the threonine (Thr) residue.
[b] Insoluble in propane-1,3-diol.
[c] PBS = phosphate-buffered saline.

the existence of a Gly residue at each row of three residues, each arising from a different peptide strand (see, for example, the DEF-molecule in Figure 2). Although all Gly residues are located near the helical axis, they are shifted by about 3 Å along the helical axis by this one-residue stagger; this permits the creation of the triple helix in the form that has the most compact packing. In accordance with Emsley et al.,[22] we have adopted the terms "leading," "middle," and "trailing" strands to represent the one-residue stagger in the triple helix. By this convention, chains E, D, and F of the DEF molecule of the PPG9-OVG peptide are the "leading," "middle," and "trailing" strands, respectively. Chain F (the trailing strand) protrudes by one residue from the middle strand (chain D) at the N-terminal side, whereas at the C-terminal side, chain F is withdrawn by one residue from the middle strand (Figure 2a).

If chain F (the trailing strand) is shifted by one triplet in the direction of the C-terminus, it becomes chain F′. In the DEF′ molecule, the one-residue stagger is in the following order: chain D, chain E, chain F′. In this molecule, chain F′ (the leading strand) is withdrawn by one residue from the middle strand (chain E) at the N-terminal side, whereas at the C-terminal side it protrudes by one residue from chain E. In the solution state, where each molecule is isolated, the DEF and DEF′ molecules cannot be discriminated, whereas in the crystal, these two molecules are not identical because each has different interactions with its neighbors. In the present study, both DEF and DEF′ molecules were observed at the same location. The difference between these two molecules is a one-triplet shift in the F chain. Experimentally, we observed two locations for both the Hyp and Val residues of the F chain in the electron-density map. We found the same type of disorder in chain E of the PPG9-OSG peptide (Figure 2b). The corresponding disordered structures are shown enclosed by rectangles in Figure 2. Although the residue numbers in chain F and chain F′ at the same row (for example, Gly 18 of chain F and Gly 15 of chain F′ in Figure 2a) are different, the atomic coordinates were assumed to be exactly the same, except for those of the five residues shown in rectangles for chains F and F′. This type of translational disorder has also been observed in the $(D\text{-Pro-}D\text{-Pro-Gly})_9$ crystal (PDB, entry 3AI6).

Packing Arrangements of the PPG9-OYG Peptides and Their Main-Chain Conformation

Although small differences were observed in the cell parameters of the PPG9-OTG, PPG9-OVG, and PPG9-OSG peptides (Table II), they were very similar to those of the $(Pro\text{-}Pro\text{-}Gly)_9$ crystal.[10] The significant deviation of the β angle of PPG-OSG from 90° appears to prevent the formation of a pseudo-merohedrally twinned crystal. The packing arrangement of these three peptide crystals was pseudo-tetrahedral, as is the case for crystals of $(Pro\text{-}Pro\text{-}Gly)_9$[10] and $(Pro\text{-}Pro\text{-}Gly)_{10}$.[23]

The triple-helical conformations of these peptides were very similar to that of $(Pro\text{-}Pro\text{-}Gly)_9$ and, therefore, close to the ideal 7/2-helical model for collagen.[24,25] The helical parameters of the host–guest regions are 52.3°/51.6° (PPG9-OTG), 52.8°/49.6° (PPG9-OVG), and 51.0°/52.5° (PPG9-OSG). Except at the peptide terminal, all the NH groups of the Gly residues were hydrogen bonded to the carbonyl oxygen atoms of the Xaa residues with an average bond length of 2.95 Å (PPG9-OTG), 2.94 Å (PPG9-OVG), or 2.94 Å (PPG9-OSG). These values are very similar to those observed in other collagen model peptides: 2.93 Å for $(Pro\text{-}Pro\text{-}Gly)_9$ and $(Pro\text{-}Hyp\text{-}Gly)_{11}$,[26] and 2.94 Å for $(Gly\text{-}Hyp\text{-}Hyp)_9$.[6]

Puckering Conformation of Hyp(X)

The χ_1 ($<NC^{\alpha}C^{\beta}C^{\gamma}$) values of Hyp residues of PPG9-OTG, PPG9-OVG, and PPG9-OSG peptides are listed in Table IV, together with those of the Yaa residues involved in the Hyp(X):Yaa(Y) stacking pairs. Because of the one-residue stagger between peptide chains, two of the Hyp13 residues face the Yaa14 residues in the adjacent chain, whereas the third Hyp13 residue faces Pro11; each molecule therefore has two Hyp13:Yaa14 stacking pairs and one Hyp13:Pro11 stacking pair (Figure 2 and Table IV).

In the PPG9-OTG structure, all the Hyp residues adopt the up-puckering conformation, except for Hyp13D (Table IV). The distance between the O^{δ} atom of Hyp13D and the C^{γ} atom of Pro17C* is 3.74 Å. Here, the asterisk denotes a residue that is generated by the symmetry operation. If Hyp13D adopted the up-puckering conformation, this dis-

Table IV Side Chain Conformations of Xaa (Hyp and Pro) and Yaa (Thr, Val, Ser, and Pro) in the Xaa:Yaa Stacking Pairs Observed in the ABC and DEF Molecules

Xaa	χ_1 (°)	Yaa	χ_1 (°)		Comment
PPG9-OTG					
Hyp13A	−21.3	Thr14C	−69.4	170.8	
Hyp13B	−27.1	Thr14A	−59.8	179.3	
Hyp13C	−13.4	Pro11B	−17.0		Hyp13C O^{δ}—Pro17D* C^{δ}, 3.77 Å[a]
Hyp13D	28.5	Thr14F	−64.8	177.1	Hyp13D O^{δ}—Pro17C* C^{γ}, 3.74 Å[a]
Hyp13E	−20.4	Thr14D	−68.4	172.2	
Hyp13F	−32.3	Pro11E	−28.3		Hyp13F O^{δ}—Pro10C* C^{β}, 3.28 Å[a]
Pro16C	30.3	Thr14B	−51.8	−172.9	
Pro16F	−17.2	Thr14E	−58.4	−174.1	Pro16F C^{γ}—Hyp13A* O^{δ}, 3.76 Å
PPG9-OVG					
Hyp13A	−19.6	Val14C	−64.6	174.7	
Hyp13B	−24.5	Pro11A	−21.0		Hyp13B O^{δ}—Pro10F* C^{β}, 4.25 Å[a]
Hyp13C	31.6	Val14B	−50.9	−175.7	Hyp13C O^{δ}—Val14F′ $C^{\gamma 2}$, 4.16 Å[a]
					Hyp13C O^{δ}—Pro17F C^{γ}, 3.60 Å[a]
Hyp13D	−17.7	Val14F[b]	−167.4	68.1	Hyp13D O^{δ}—Pro16B* C^{β}, 4.17 Å[a]
Hyp13D	−17.7	Pro11F′[b]	19.8		Hyp13D O^{δ}—Pro16B* C^{β}, 4.17 Å[a]
Hyp13E	−25.3	Val14D	−175.6	62.0	Val14D $C^{\gamma 1}$—Pro10E* C^{β}, 3.68 Å
					Val14D $C^{\gamma 1}$—Pro11E* C^{δ}, 3.76 Å
Hyp13F[b]	28.3	Pro11E	−24.7		Hyp13F O^{δ}—Pro17C C^{γ}, 3.28 Å[a]
Hyp13F′[b]	−11.9	Val14E	−61.6	176.7	
Pro16B	8.6	Val14A	−58.4	−179.4	
Pro16D	30.9	Val14F′[b]	−64.7	177.8	
PPG9-OSG					
Hyp13A	−24.6	Ser14C	−59.8		Hyp13A O^{δ}—Ser14B* O^{γ}, 2.70 Å
					Hyp13A O^{δ}—Ser14B′* O^{γ}, 3.41 Å
Hyp13B	−17.0	Ser14A	−73.7		
Hyp13C	−20.4	Pro11B	−27.7		Hyp13C O^{δ}—Pro13D C^{β}, 4.13 Å[a]
Hyp13D	−23.5	Ser14F	−62.4		
Hyp13E[c]	−17.7	Pro11D	−23.2		
Hyp13E′[c]	−10.9	Ser14D	−66.6		
Hyp13F	31.0	Ser14E[c]	−64.0		
Hyp13F	31.0	Pro11E′[c]	−8.9		
Pro16C	26.5	Ser14B[d]	−49.9		Ser14B O^{γ}—Hyp13A* O^{δ}, 2.70 Å
					Pro16C C^{β}—Hyp13E O^{δ}, 3.47 Å
Pro16C	26.5	Ser14B′[d]	65.0		Ser14B′ O^{γ}—Hyp13A* O^{δ}, 3.41 Å

[a] The distance would become shorter than the sum of the van der Waals radii of the corresponding atoms if Hyp13 adopted the opposite puckering conformation.

[b] The F-chain of PPG9-OVG has a translational disorder along the helical axis with one triplet.

[c] The E-chain of PPG9-OSG has a translational disorder along the helical axis by one triplet (Figure 2b). Therefore, the site of Hyp13E is also occupied by Pro10E′ and the site of Pro16E is occupied by Hyp13E′. The site occupancy factors of the E- and E′-chains are 0.55 and 0.45, respectively.

[d] The Ser14 residue in the B-chain of PPG9-OSG is a mixture of Ser14B and Ser14B′ with g^+ and g^- side chain conformations, respectively.

* Denotes that this chain was generated from the original by means of crystallographic symmetry.

tance would be less than the sum of the van der Waals radii of the corresponding atoms. The Hyp13D is therefore forced to adopt a down-puckering conformation. However, in aqueous solution, where no triple helix interacts with its surrounding molecules, Hyp13D can adopt an up-puckering conformation like those of the other three Hyp13 residues involved in the Hyp13:Thr14 stacking pairs. The up-puckering conformations of Hyp13C and Hyp13F are contrary to our previous hypothesis[11,12] that the Hyp(X) residue involved in the Hyp(X):Pro(Y) stacking pair adopts a down-puckering conformation. However, if these Hyp13 residues were to adopt the down-puckering conformation, the atomic distances between the O^{δ} atom of Hyp13 and the Pro residues in adjacent molecules would become shorter than the sum of the van der Waals radii of the corresponding atoms (Table IV). In an aqueous solution, these Hyp13 residues will adopt a down-puckering conformation, for the same reasons as discussed above.

In the PPG9-OVG structure, of the five Hyp13 residues that are involved in Hyp13:Val14 stacking pairs (including the disordered Hyp13F′ residue), four adopt an up-puckering conformation and Hyp13C adopts a down-puckering conformation (Table IV). If the Hyp13C residue were to adopt the up-puckering conformation, the distance between the O^{δ} atom of Hyp13C and the $C^{\gamma 2}$ atom of Val14F′ (or the C^{γ} atom of Pro17F) would be less than the sum of the van der Waals radii of the corresponding atoms (Table IV). The residue is therefore forced to adopt the down-puckering conformation. Here, both the Pro17F and Val14F′ residues are the counterparts of the disordered residues (Figure 2a). In an aqueous solution, it is quite reasonable to assume that the Hyp13C residue adopts an up-puckering conformation like those of the other four residues in the Hyp13:Val14 stacking. Although the puckering conformation of Hyp13F is consistent with our previous hypothesis,[12] that of two residues (Hyp13B and Hyp13D) contravenes it. This can be attributed to the short contacts between the O^{δ} atom of Hyp13B and the C^{β} atom of Pro10F*, and between the O^{δ} atom of Hyp13D and the C^{β} atom of Pro16B* when the Hyp13B and Hyp13D residues adopt the down-puckering conformation (Table IV).

In the PPG9-OSG structure, of the five Hyp13 residues that are involved in the Hyp13:Ser14 stacking pairs (including the disordered Hyp13E′ residue), four adopt the up-puckering conformation, whereas Hyp13F adopts the down-puckering conformation (Table IV). In the last case, there is no attractive interaction with this residue. Furthermore, there is no short contact with adjacent molecules when the Hyp13F residue adopts an up-puckering conformation. Because of the translational disorder in the E chain, the Hyp13F residue has two different stacking pairs, Hyp13F:Ser14E and Hyp13F:Pro11E′ (Table IV). The down-puckering conformation of the Hyp13F residue may therefore be due to the stronger effect of the Hyp13F:Pro11E′ stacking pair, rather than to the effect of Hyp13F:Ser14E. On the other hand, despite the presence of sufficient space to allow both up- and down-puckering conformations, the Hyp13E residue that is involved in the Hyp13E:Pro11D stacking pair adopts an up-puckering conformation, contrary to our previous hypothesis.[12] So far, this is the only case of a Hyp(X):Pro(Y) stacking pair in which the adoption of an up-puckering conformation by the Hyp(X) residue cannot be rationalized. The disordered structure of the E chain may have some effect on the unexpected puckering conformation of Hyp13E residue. These facts show that the Hyp(X) residues that are involved in the Hyp(X):Thr(Y), Hyp(X):Val(Y) and Hyp(X):Ser(Y) stacking pairs generally adopt an up-puckering conformation, which is the intrinsic preference for Hyp residues, but conflicts with the positional preference for the X.

Unique Side-Chain Conformations of Thr, Val, and Ser Residues in Triple Helices

Generally, the side chains of Thr, Val, and Ser residues adopt one of three conformations: *trans* (*t* for short), *gauche*$^{+}$ (g^{+}), or *gauche*$^{-}$ (g^{-}). These are defined by χ_1 and are denoted as either <N–C^{α}–C^{β}–C^{γ} or <N–C^{α}–C^{β}–O^{γ}. In the case of Thr and Val residues, depending on the combination of the two atoms attached to the C^{β} atom (C^{γ} and O^{γ} in Thr or $C^{\gamma 1}$ and $C^{\gamma 2}$ in Val), the three conformations are referred to as t-g^{-}, g^{+}-t, and g^{-}-g^{+}. The proportions of these three conformations found in various compounds whose details have been deposited in the Cambridge Structural Database (CSD)[3] are shown in Figure 3. The total numbers of compounds used to generate these statistics were 106 for Thr, 1039 for Val, and 166 for Ser. Although the population of the t-g^{-} (or t) conformation is rather low in all cases (see Figure 3), there is no tendency to prefer one particular conformation.

Because each asymmetric unit of the three PPG9-OYG crystals contains two triple helices (six peptide strands), there are six independent Yaa residues. Table V shows the χ_1 values of the Thr, Val, and Ser residues observed in this study. In the PPG9-OTG crystal, all six Thr residues adopted the g^{+}-t conformation (100%). Although the Val residue in the D chain and one of the disordered Val residues in the F chain of PPG9-OVG adopt the t-g^{-} conformation, the other five Val residues adopt the g^{+}-t conformation (75%). The t-g^{-} conformation of Val14D and Val14F may be the result of the attractive interaction between the $C^{\gamma 1}$ atoms of these residues and the carbon atoms of adjacent molecules (Table V). Therefore, we expected that these residues would adopt the g^{+}-t conformation in an aqueous solution where there is no such attractive interaction. In the PPG9-OSG crystal, one of the disordered Ser residues in the B-chain (Ser14B′) adopted the g^{-} conformation, whereas all other residues adopted the g^{+} conformation (92%). Taking into account the tendency observed in the CSD analysis (see Figure 3) and the results obtained in the present study, we concluded that, in the triple-helical structures of PPG9-OYG peptides, Thr, Val, and Ser residues in the Y position have a strong preference toward adopting the g^{+}-t (or g^{+}) conformation.

Why is the g^{+}-t Conformation Favored in the Hyp(X):Val(Y) and Hyp(X):Thr(Y) Stacking Pairs?

As typical examples of Hyp(X):Yaa(Y) stacking pairs, the structures of the Hyp13A:Val14C, Hyp13B:Thr14A, and Hyp13A:Ser14C stacking pairs are shown in Figures 4a, 5a, and 6a, respectively. Here, the Val14C and Thr14A residues adopt the g^{+}-t conformation and the Ser14C residue adopts the g^{+} conformation. For the sake of comparison, the t-g^{-}

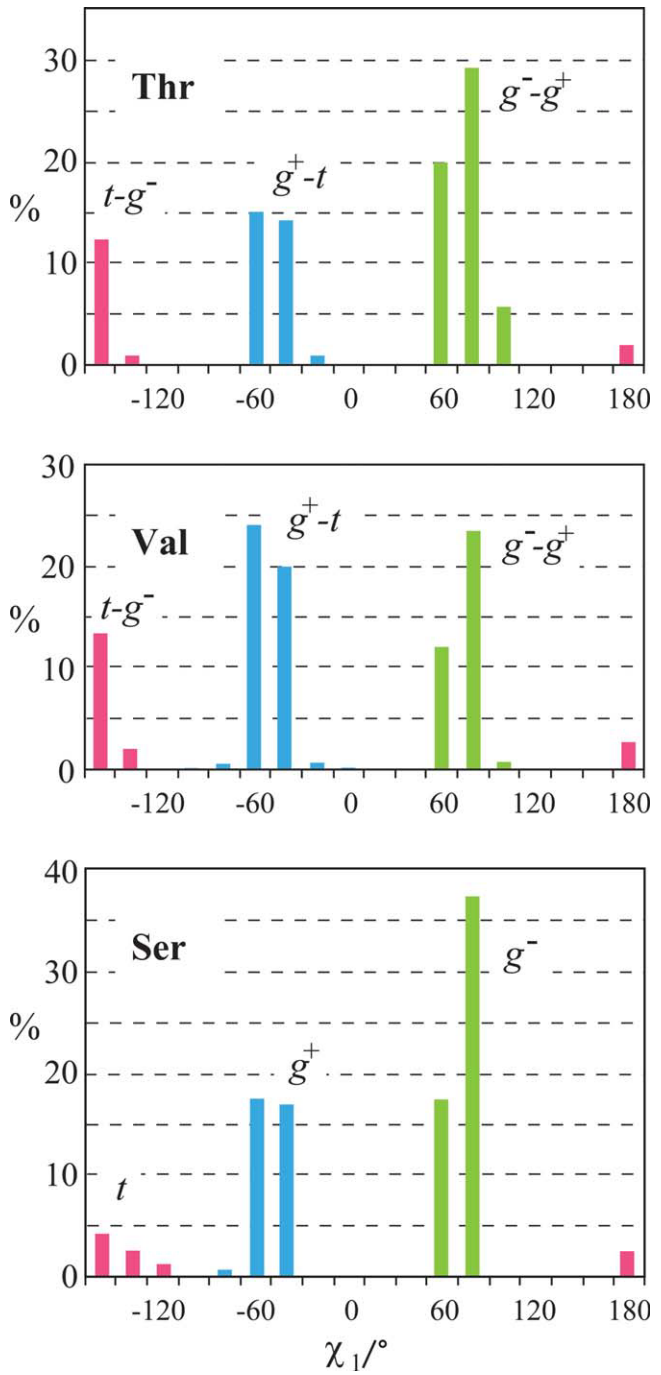

FIGURE 3 Distributions of side-chain conformations of Thr, Val, and Ser residues, as obtained from the Cambridge Structural Database (CSD). The numbers of compounds used in calculating these distributions were 106 for Thr, 1039 for Val, and 166 for Ser residues.

and g^--g^+ conformations of the PPG9-OVG peptide are also shown in Figures 4b and 4c, respectively. These were generated by rotating the dimethyl group by ±120° around the C^α–C^β bond of Val14C from the location of the g^+-t conformation (Figure 4a). In the g^+-t conformation, both the $C^{\gamma 1}$ and $C^{\gamma 2}$ atoms face the ring plane of Hyp13A and make van der Waals contacts with it. For example, the distance from C^β of Hyp13A to $C^{\gamma 1}$ of Val14C is 4.75 Å, that from C^γ of Hyp13A to C^β of Val14C is 4.67 Å, that from C^γ of Hyp13A to $C^{\gamma 2}$ of Val14C is 3.76 Å, and that from C^δ of Hyp13A to $C^{\gamma 2}$ of Val14C is 4.06 Å. On the other hand, in the t-g^- and g^--g^+ conformations, one of the C^γ atoms of the Val14C residue is not close to the Hyp residue, which diminishes the van der Waals contact with the proline ring and increases the surface area of the Val14C that is exposed to the solvent water. We believe that this van der Waals stacking interaction between Hyp(X) and Val(Y) residue is the reason why Val residues prefer the g^+-t conformation when they face each other in the triple-helical structure. By analogy to the Hyp(X):Val(Y) stacking pair, the conformation of the Thr residues involved in the Hyp(X):Thr(Y) stacking pair is expected to adopt the same g^+-t conformation, because the difference between Thr and Val residues is whether the C^β atom is connected to two methyl groups or to one methyl group and one hydroxy group. In fact, the structure of the Hyp13B:Thr14A stacking pair obtained in the present analysis (Figure 5a) showed that the side-chain arrangement of the Thr14A residue is very similar to that of the Val14C residue (Figure 4a).

To explain the stabilization mechanism of Hyp residues in the X position of the $(Gly\text{-}Hyp\text{-}Hyp)_9$ and $(Hyp\text{-}Hyp\text{-}Gly)_{10}$ peptides, Improta et al.[27] identified the importance of the contribution of dipole–dipole interactions between the two C^γ–O^δ groups in the Hyp(X):Hyp(Y) stacking pairs. In the

Table V χ_1 **Values (Degrees) of Thr, Val, and Ser in the Y Position of the PPG9-OYG Peptide**

	Thr		Val		Ser
Chain	χ_1 (O^γ)	χ_1 (C^γ)	χ_1 ($C^{\gamma 2}$)	χ_1 ($C^{\gamma 1}$)	χ_1 (O^γ)
A	−59.8	179.3	−58.0	−179.4	−73.7
B	−51.8	−172.9	−50.9	−175.7	−49.4
B′					65.0
C	−69.4	170.8	−64.6	174.7	−59.8
D	−68.4	172.2	−175.6[a]	62.0[a]	−66.6
E	−58.4	−174.1	−61.6	176.7	−64.0
E′					−41.7
F	−64.8	177.1	−167.4[b]	68.1[b]	−62.4
F′			−64.7	177.8	

[a] The $C^{\gamma 1}$ atom of Val14D has intermolecular contacts with C^β (3.68 Å) of the Pro10E* residue and C^δ (3.76 Å) of the Pro11E* residue. Here, * denotes that the chain was generated from the original by means of crystallographic symmetry.

[b] The $C^{\gamma 1}$ atom of Val14F has an intermolecular hydrophobic interaction with C_β (4.24 Å), $C^{\gamma 1}$ (4.50 Å), and $C^{\gamma 2}$ (4.63 Å) of Val14C in the same asymmetric unit.

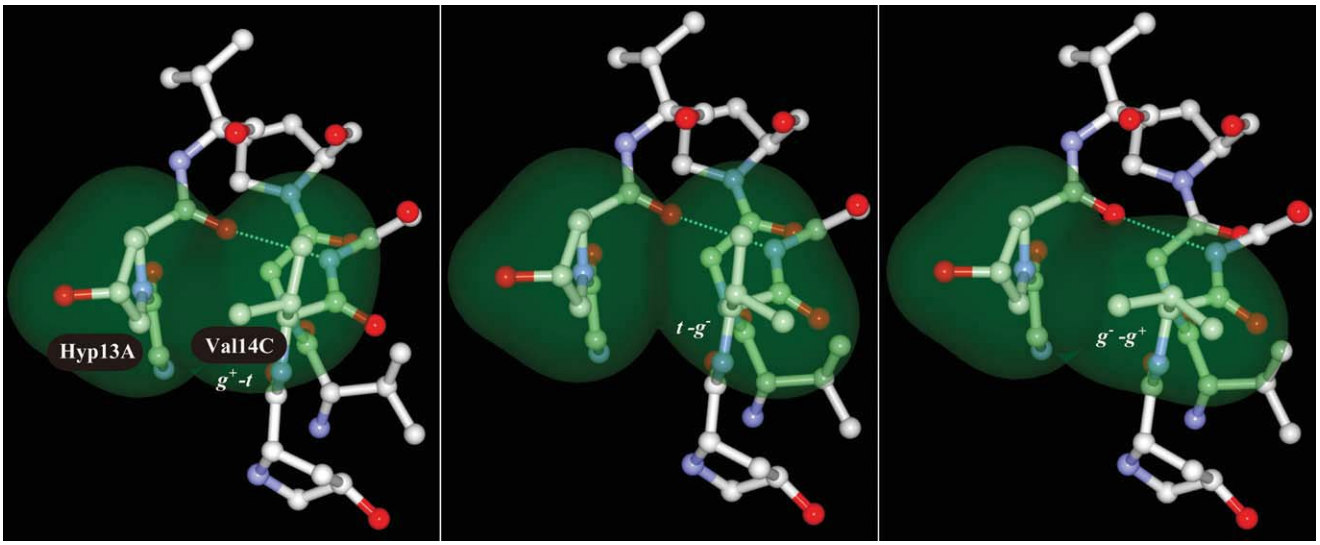

FIGURE 4 Structures of Hyp(X):Val(Y) stacking pairs with three different side-chain conformations. (a) The g^+-t conformation of the Val residue in the Hyp13A:Val14C stacking pair as observed in the PPG9-OVG crystal. (b) The t-g^- conformation and (c) the g^--g^+ conformation generated from the g^+-t conformation (a) by rotating the dimethyl group around the C^α–C^β bond. The C^β, C^γ, C^δ, and O^δ atoms of the Hyp residue and the C^β, $C^{\gamma 1}$, and $C^{\gamma 2}$ atoms of the Val residue are shown by the translucent green van der Waals spheres. The interchain hydrogen bond between the NH group of Gly and the CO group of the Xaa residues is shown as a dotted line.

same manner, we expect that a similar dipole–dipole interaction between the C^γ–O^δ group of Hyp and the C^β–O^γ group of the Thr residues will contribute to the stabilization of the triple-helix, in addition to the van der Waals stacking interaction. Because this dipole–dipole interaction is most effective when the C^γ–O^δ group of Hyp and the C^β–O^γ group of Thr residues adopt a head-to-tail arrangement, only the g^+-t conformation is preferred. Therefore, the g^+-t conformation is preferable for both the van der Waals interaction and the dipole–dipole interaction. On the other hand, for the *allo*Thr

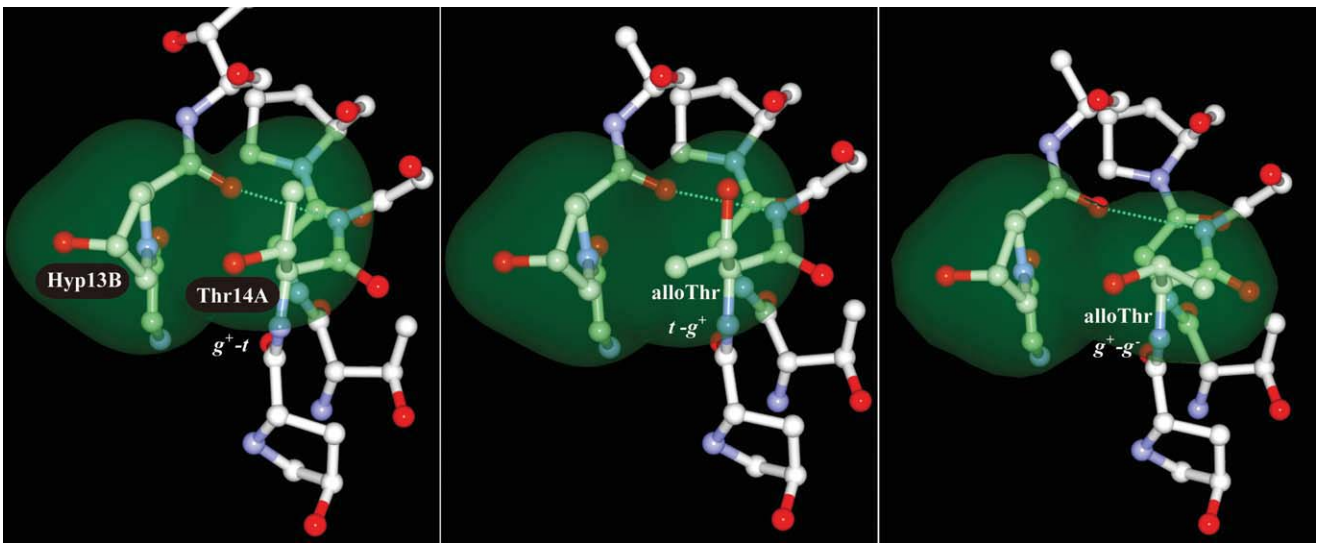

FIGURE 5 (a) The g^+-t conformation of the Thr residues involved in the Hyp13B:Thr14A stacking pair observed in the PPG9-OTG crystal. (b) The t-g^+ conformation of the *allo*Thr residue, generated by changing the location of the O^γ and C^γ atoms of the Thr residue in (a). (c) The g^+-g^- conformation of the *allo*Thr residue generated from (b) by rotating the side chain around the C^α–C^β bond. The C^β, C^γ, C^δ, and O^δ atoms of the Hyp residue and the C^β, C^γ, and O^γ atoms of the Thr and *allo*Thr residues are shown by the translucent green van der Waals spheres.

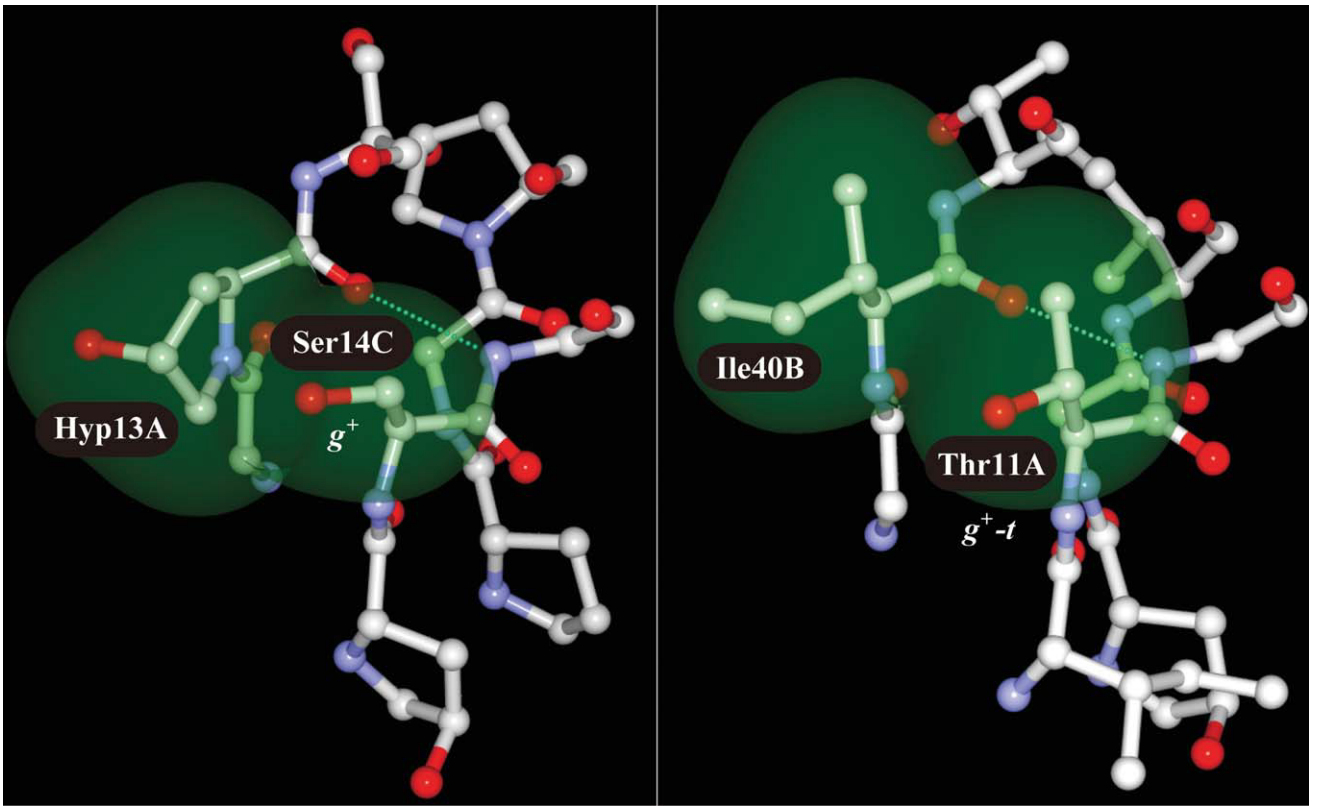

FIGURE 6 (a) The g^+ conformation of the Ser residue involved in the Hyp13A:Ser14C stacking pair observed in the PPG9-OSG crystal. (b) The g^+-t conformation of the Thr residues involved in the Ile40B:Thr11A stacking pair of T3-785 peptide[28] (PDB entry; 1BKV). The C^β, C^γ, C^δ, and O^δ atoms of the Hyp residue and the C^β and O^γ atoms of the Ser residue (a), and the C^β, C^γ, and O^γ atoms of the Thr residue and the C^β, $C^{\gamma 1}$, and $C^{\gamma 2}$ atoms of the Ile residue (b) are shown by the translucent green van der Waals spheres.

residue, the g^+-g^- conformation is most favorable for the dipole–dipole interaction (Figure 5c), whereas this conformation is not suitable for the van der Waals stacking interaction because the methyl group is located away from the Hyp residue. For the van der Waals interaction, the t-g^+ conformation is the best (Figure 5b). Therefore, in the case of *allo*Thr, the favorable conformations for the two types of interaction conflict with one another. This explains why Ac-(Gly-Hyp-Thr)$_{10}$-NH_2 peptide forms a triple helix, whereas Ac-(Gly-Hyp-*allo*Thr)$_{10}$-NH_2 peptide does not. [8]

Because Ser residues have only one group bonded to the C^β atom, it is obvious that the g^+ conformation is preferred for both the van der Waals interaction and the dipole–dipole interaction, as can be seen in Table V and Figure 6a. However, judging from the T_m values of the PPG9-OTG, PPG9-OVG, and PPG9-OSG peptides (Table III), it appears that the triple-helix is not well stabilized when only the hydroxy group of the Ser residue is involved.

The conclusions drawn in the above discussion are further confirmed by the crystal structures of related peptides. Other than the PPG9-OTG peptide (1.08 Å resolution) of the present study, the crystal structure of the T3-785 peptide[28] (PDB entry: 1BKV; 2 Å resolution) is the only one in which the Thr side-chain conformation is reported at a resolution of better than 3 Å. In this crystal, there are three Thr residues in an asymmetric unit. Two of them are involved in the Ile(X):Thr(Y) stacking pair and adopt a g^+-t conformation (67%), whereas the third, which is involved in an Ala(X):Thr(Y) stacking pair, adopts a g^--g^+ conformation. The stacking interaction with the single C^β atom of the Ala residue was not sufficient for the Thr side chain to result in adoption of the g^+-t conformation, whereas the interaction with the C^β and C^γ atoms of the Ile residues appear to be sufficient to result in adoption of the g^+-t conformation (Figure 6b).

Triple-Helix Stabilization By the Hyp(X):Thr(Y) and Hyp(X):Val(Y) Stacking Pairs

From their measurements of the T_m of Ac-(Gly-Hyp-Yaa)$_{10}$-NH_2 peptides (Yaa = Thr, Val, Ser, Ala, *allo*Thr), Mizuno et

al.[8] concluded that the stereochemical configuration of the both hydroxy and methyl groups of the Thr residue is critical in stabilizing the triple-helix. Furthermore, to explain the stability of the Ac-(Gly-Hyp-Thr)$_{10}$-NH$_2$ peptide, Mizuno et al. hypothesized that the methyl group of the Thr residue shields the interchain hydrogen bond between the Gly and the Xaa residues from solvent water. On the basis of a MD simulation, Radmer et al.[15] reported that this solvent shielding does not provide an adequate explanation for the stability of the peptide, and they attributed the origin of the unstable triple-helices of the *allo*Thr-, Ser- and Ala-containing peptides to weakening of the interchain hydrogen bonds as a result of the extended Yaa residue ψ-angles, which prevents the attainment of the optimal geometry.[15]

The host–guest peptides PPG9-OYG (Yaa = Thr, Val, Ser) showed the same tendency in terms of triple-helix stability as Ac-(Gly-Hyp-Yaa)$_{10}$-NH$_2$ peptides (Table I). According to the high-resolution crystal structures, the side chains of the Yaa residues in the PPG9-OYG peptides adopt a unique g^+-*t* (or g^+) conformation that optimizes both the van der Waals interactions and the dipole–dipole interactions between stacking pairs. In the case of the Thr residue, the g^+-*t* conformation favors both the van der Waals interaction and the dipole–dipole interaction, whereas in the case of the *allo*Thr residue, no conformation favors both these interactions. This finding explains why the *allo*Thr-containing peptide is less stable than the Thr-containing peptide, and it supports Mizuno's conclusion that the stereochemical configuration of both the hydroxy and the methyl groups of the Thr residue is essential for stabilization of the triple helix.

Because the Ser residue has only one group (OH) attached to the C$^\beta$ atom, the van der Waals interaction between the Hyp(X) and Ser(Y) residues in the Hyp(X):Ser(Y) stacking pair is weaker than the corresponding interactions in the Hyp(X):Thr(Y) and Hyp(X):Val(Y) stacking pairs. Therefore, it is obvious that the triple helix of the PPG9-OSG is less stable than those of PPG9-OTG and PPG9-OVG, which, in turn, explains the inability of Ac-(Gly-Hyp-Ser)$_{10}$-NH$_2$ to form a triple helix in aqueous solution.[8] Similarly, the van der Waals interaction between Hyp(X) and Ala(Y) is considerably weakened because there is no group attached to the C$^\beta$ atom of the Ala residue, which explains the inability of the Ac-(Gly-Hyp-Ala)$_{10}$-NH$_2$ peptide to form a triple helix.[8]

Because we had high-resolution structures for PPG9-OYG (Y = T, V, S) peptides, we examined the proposals of Radmer et al.[15] that (1) unstable molecules have weaker interchain NH(Gly)—CO(Xaa) hydrogen bonds, and (2) the weakened hydrogen bonds result from extended Yaa residue ψ-angles. In the present study, the average ψ values of Yaa residues are 149.2° for Ser in PPG9-OSG, 138.9° for Thr in PPG9-OTG, and 142.3° for Val in PPG9-OVG. In agreement with the proposals of Radmer et al.,[15] we observed a rather large ψ value for the Ser residue in comparison with those of the Thr and Val residues. However, this value was very close to the average ψ value for Pro in the Y position of PPG9-OTG (150.2°), PPG9-OVG (152.5°), and PPG9-OSG (151.0°), and also close to those for (Pro-Hyp-Gly)$_{11}$ (149.6°) and (Pro-Hyp-Gly)$_{10}$ (150.0°).[26] Furthermore, the average hydrogen-bond lengths between the NH group of Gly and the CO group of Xaa in the adjacent chain were not significantly different for these three peptides. For example, for PPG9-OTG, the total average hydrogen-bond distance and the average hydrogen-bond distance of the guest Hyp-Yaa-Gly regions are 2.95 and 2.91 Å, respectively; for PPG9-OVG, they are 2.94 and 2.93 Å, respectively; and for PPG9-OSG, they are 2.94 and 2.93 Å, respectively. At least in the single-crystal structures of these peptides, no relationship was found between the ψ values of the Yaa residues and the strengths of the interchain hydrogen bonds.

In conclusion, we analyzed the single-crystal structures of PPG9-OTG, PPG9-OVG, and PPG9-OSG peptides at a high resolution (better than 1.2 Å). On the basis of these structures, we were able to provide a clear explanation of the difference in the triple-helical stability of peptides containing the Hyp-Thr-Gly, Hyp-Val-Gly, and Hyp-Ser-Gly sequences. The triple-helix stability of these peptides depends on the van der Waals and/or the dipole–dipole interactions in the Hyp(X):Yaa stacking pairs. This idea also explains the inability of Ac-(Gly-Hyp-*allo*Thr)$_{10}$-NH$_2$ and Ac-(Gly-Hyp-Ala)$_{10}$-NH$_2$ to form triple helices in water, as observed by Mizuno et al.[8]

The authors thank the staff of the Osaka University beamline BL44XU at SPring-8 for collecting data for the PPG9-OVG and PPG9-OSG crystals. The crystallization and X-ray data acquisition for the PPG9-OTG peptide were performed by the staff of PharmAxess Inc. (Tokyo). This work was supported in part by a Grant-in-Aid for Scientific Research (B) from the Japan Society for the Promotion of Science (to K.O.) and a grant by Shriners Hospital (to H.P.B.).

REFERENCES

1. Inouye, K.; Kobayashi, Y.; Kyogoku, Y.; Kishida, Y.; Sakakibara, S.; Prockop, D. J. Arch Biochem Biophys 1982, 219, 198–203.
2. Berman, H. M.; Battistuz, T.; Bhat, T. N.; Bluhm, W. F.; Bourne, P. E.; Burkhardt, K.; Feng, Z.; Gilliland, G. L.; Iype, L.; Jain, S.; Fagan, P.; Marvin, J.; Padilla, D.; Ravichandran, V.; Schneider, B.; Thanki, N.; Weissig, H.; Westbrook, J. D.; Zardecki, C. Acta Crystallogr D Biol Crystallogr 2002, 58, 899–907.
3. Allen, F. H.; Bellard, S.; Brice, M. D.; Cartwright, B. A.; Doubleday, A.; Higgs, H.; Hummelink, T.; Hummelinkpeters, B. G.; Kennard, O.; Motherwell, W. D. S.; Rodgers, J. R.; Watson, D. G. Acta Crystallogr Sect B Struct Sci 1979, 35, 2331–2339.

4. Vitagliano, L.; Berisio, R.; Mazzarella, L.; Zagari, A. Biopolymers 2001, 58, 459–464.
5. Kawahara, K.; Nishi, Y.; Nakamura, S.; Uchiyama, S.; Nishiuchi, Y.; Nakazawa, T.; Ohkubo, T.; Kobayashi, Y. Biochemistry 2005, 44, 15812–15822.
6. Schumacher, M.; Mizuno, K.; Bächinger, H. P. J Biol Chem 2005, 280, 20397–20403.
7. Berisio, R.; Granata, V.; Vitagliano, L.; Zagari, A. J Am Chem Soc 2004, 126, 11402–11403.
8. Mizuno, K.; Hayashi, T.; Bächinger, H. P. J Biol Chem 2003, 278, 32373–32379.
9. Bhatnagar, R. S.; Pattabiraman, N.; Sorensen, K. R.; Langridge, R.; MacElroy, R. D.; Renugopalakrishnan, V. J Biomol Struct Dyn 1988, 6, 223–233.
10. Hongo, C.; Noguchi, K.; Okuyama, K.; Tanaka, Y.; Nishino, N. J Biochem 2005, 138, 135–144.
11. Okuyama, K.; Hongo, C.; Wu, G.; Mizuno, K.; Noguchi, K.; Ebisuzaki, S.; Tanaka, Y.; Nishino, N.; Bächinger, H. P. Biopolymers 2009, 91, 361–372.
12. Okuyama, K.; Morimoto, T.; Narita, H.; Kawaguchi, T.; Mizuno, K.; Bächinger, H. P.; Wu, G.; Noguchi, K. Acta Cryst 2010, D66, 88–96.
13. Goldstein, A.; Adams, E. J Biol Chem 1970, 245, 5478–5483.
14. Muir, L.; Lee, Y. C. J Biol Chem 1970, 245, 502–509.
15. Radmer, R. J.; Klein, T. E. Biophys J 2006, 90, 578–588.
16. Jiravanichanun, N.; Mizuno, K.; Bächinger, H. P.; Okuyama, K. Polym J 2006, 38, 400–403.
17. Otwinowski, Z.; Minor, W. Macromol Crystallogr 1997, 276, 307–326.
18. Adams, P. D.; Grosse-Kunstleve, R. W.; Hung, L. W.; Ioerger, T. R.; McCoy, A. J.; Moriarty, N. W.; Read, R. J.; Sacchettini, J. C.; Sauter, N. K.; Terwilliger, T. C. Acta Cryst 2002, D58, 1948–1954.
19. Mccoy, A. J.; Grosse-Kunstleve, R. W.; Adams, P. D.; Winn, M. D.; Storoni, L. C.; Read, R. J. J Appl Cryst 2007, 40, 658–674.
20. Sheldrick, G. M. Acta Cryst 2008, A64, 112–122.
21. Emsley, P.; Cowtan, K. Acta Cryst 2004, D60, 2126–2132.
22. Emsley, J.; Knight, C. G.; Farndale, R. W.; Barnes, M. J.; Liddington, R. C. Cell 2000, 101, 47–56.
23. Berisio, R.; Vitagliano, L.; Mazzarella, L.; Zagari, A. Protein Sci 2002, 11, 262–270.
24. Okuyama, K.; Xu, X.; Iguchi, M.; Noguchi, K. Biopolymers 2006, 84, 181–191.
25. Okuyama, K.; Takayanagi, M.; Ashida, T.; Kakudo, M.; Sakakibara, S.; Kishida, Y. Polym J 1977, 9, 341–343.
26. Okuyama, K.; Hongo, C.; Fukushima, R.; Wu, G.; Narita, H.; Noguchi, K.; Tanaka, Y.; Nishino, N. Biopolymers 2004, 76, 367–377.
27. Improta, R.; Berisio, R.; Vitagliano, L. Protein Sci 2008, 17, 955–961.
28. Kramer, R. Z.; Bella, J.; Brodsky, B.; Berman, H. M. J Mol Biol 2001, 311, 131–147.

Reviewing Editor: David A. Case